ChemComm

Accepted Manuscript

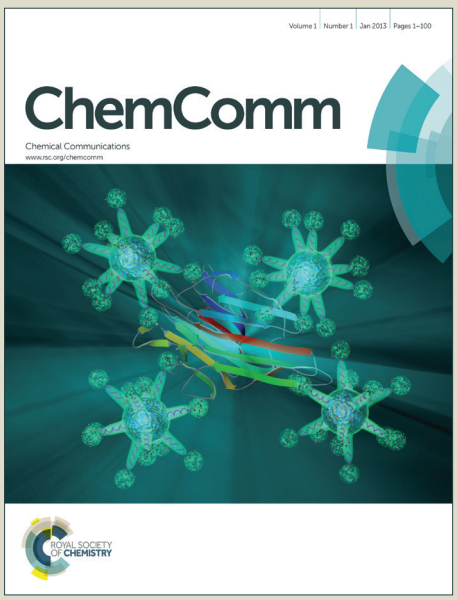

ROYAL SOCIETY OF CHEMISTRY

www.rsc.org/chemcomm

View Article Online
DOI: 10.1039/C5CC04317D

Chemical Communications

COMMUNICATION

On-surface photo-dissociation of C-Br bonds: towards room temperature Ullmann coupling

Received 00th January 20xx,

Andrea Basagni,*[a] Lara Ferrighi,[b] Mattia Cattelan,[a] Louis Nicolas,[c] Karsten Handrup,[d] Luca Vaghi,[b] Antonio Papagni,[b] Francesco Sedona,*[a] Cristiana Di Valentin,[b] Stefano Agnoli[a] and Mauro Sambi[a]

Accepted 00th January 20xx

DOI: 10.1039/x0xx00000x

www.rsc.org/

The surface-assisted synthesis of gold-organometallic hybrids on the Au (111) surface is reported both by thermo- and light-initiated dehalogenation of bromo-substituted tetracene. Combined X-ray photoemission (XPS) and scanning tunneling microscopy (STM) data reveal a significant increase of the surface order when mild reaction conditions are combined with 405 nm light irradiation.

The bottom-up synthesis of covalently bonded organic nanostructures has recently emerged as a very promising way to obtain surface-supported one-dimensional molecular wires,[1] nanoribbons,[2] or two dimensional networks.[3]

Among the various coupling,[4] Ullmann polymerization has proven to be a versatile approach to the covalent networks formation, since the topology of the resulting scaffold can be tuned simply by changing the position and/or the chemical identity of the halogen atoms within the molecular precursor.[5]

The Ullmann reaction starts with an initial surface-assisted homolytic dissociation of the C-X bond, followed by the reversible formation of an organometallic framework based on carbon-metal-carbon bonds. The (111) surface of Cu, Ag and Au are the most studied substrates for two dimensional Ullmann-like coupling reactions. On Cu and Ag the de-halogenation is already active at room temperature (RT)[6,7] or can be activated with a mild annealing,[8] whereas on Au it is necessary to anneal at more than 120°C to break the C-Br bond.[9] On Cu and Ag, in order to complete the covalent coupling by removing the bridging metal atoms, a thermal treatment at relatively high temperature is required. This treatment in certain cases leads to molecular desorption or to the partial decomposition of the precursor, especially in the case of thermolabile substances.[10] By contrast, this step on Au is already activated at RT. The metal-organic intermediate is not observed after the de-halogenation: the final covalently linked structure is directly obtained.[11] Indeed, until now only few examples of stable Au organometallic chains have been reported.[12,13] In these cases sterically hindered monomers have been used in order to prevent the elimination of the metal atom and the formation of the C-C bond.

Surface poisoning by the chemisorbed halogen species can also hinder the long range ordering of the self-assembled structures and, again, this effect is more pronounced on Cu and Ag than on Au.[10,14] For these reasons and for the higher diffusivity of surface stabilized radicals on Au with respect to other transition metals, Au surfaces are frequently used in this field. However, since the dehalogenation step is expected to be the rate limiting one,[14] due to the lower catalytic activity of gold, a non-thermal activation is required to polymerize the precursors in sufficiently mild conditions to preserve the molecular organization and the chemical identity of the precursor.

Recently, the photochemical activation of specific functional groups has proven to be an alternative tool to stabilize the self-organized structures without disrupting the long-range order.[15,16] In this communication we provide unambiguous evidence for the photochemical dissociation of the C-Br bond, that is the rate determining step for the Ullmann-like coupling on Au surfaces, by combining scanning tunneling microscopy (STM) with surface averaging and chemically sensitive techniques. Differently from previous studies on surface-confined covalent coupling, in which the occurrence of the photo-dissociation and of the polymerization was postulated exclusively on the basis of local probe measurements,[17] our sterically hindered precursor (5,11-dibromo-tetracene, DBT hereafter) allows us to observe specific spectroscopic and topological fingerprints associated with the

[a] Department of Chemical Sciences, University of Padova, Via Marzolo 1, 35131 Padova (Italy).
E-mail: andrea.basagni@studenti.unipd.it
francesco.sedona@unipd.it
[b] Department of Materials Science, University of Milano-Bicocca, Via Cozzi 55, 20125 Milano (Italy).
[c] Ecole Normale Supérieure de Cachan 61, avenue du Président Wilson, 94235 Cachan cedex (France).
[d] MAX IV Laboratory, Lund University, Box 118, SE-22100 Lund, Sweden.

†Electronic Supplementary Information (ESI) available: Additional simulations data and Experimental details. See DOI: 10.1039/x0xx00000x

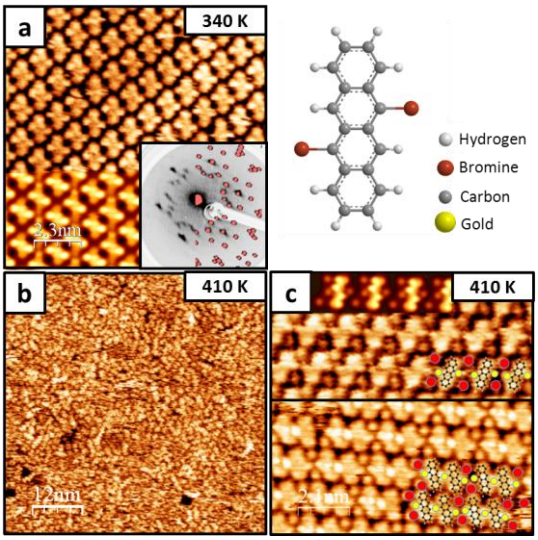

Figure 1: STM images of the dark area: **a)** monolayer of DBT molecules deposited on Au (111) with superimposed DFT simulation (inset: 17 eV experimental and $\begin{pmatrix} 3 & 3.5 \\ 0 & 5 \end{pmatrix}$ simulated LEED patterns); **b)** representative image of the surface after annealing at 410 K; **c)** zoom-in of one of the rare ordered areas obtained after annealing at 410 K; the superimposed models highlight the presence of the organometallic dimers and of the chemisorbed bromine. Tunneling parameters are a) I= 3 nA, V_{bias}= 0.67 V; b) I= 2.5 nA, V_{bias}= -0.52 V; c) I^{upper}= 1.5 nA, V^{upper}_{bias}= 0.69 V; I^{bottom}= 3.6 nA, V^{bottom}_{bias}= -0.1 V.

organometallic intermediates obtained after the C-Br homolytic dissociation. This is possible because the steric repulsion among peripheral H atoms of adjacent molecules hampers the in-plane coupling of the monomers.[18]

Figure 1a is a STM image of a full monolayer of DBT after thermal desorption of the partially formed second layer at 340 K, showing the Au (111) surface covered by a well-organized superstructure whose periodicity is described by the $\begin{bmatrix} 3 & 3.5 \\ 0 & 5 \end{bmatrix}$ epitaxial matrix, as confirmed by the LEED pattern. The main molecular axis lies along the $\langle 1\bar{1}0 \rangle$ substrate direction and, according to the DFT simulated unit cell, each Br substituent can interact attractively with a partial positive charge residing on an H atom of the adjacent molecule to form a Br---H intermolecular interaction, $d_{Br\cdots H}$≈3.3 Å, which favours the formation of an ordered network.[19] At RT the Au herringbone reconstruction is neither modified nor lifted upon adsorption of the molecules, indicating a weak molecule–substrate interaction. DFT calculations of a physisorbed monolayer provide a distance from the substrate of 3.2 Å and a binding energy of 2.0 eV per DBT, typical of a weakly interacting system driven by Van der Waals forces and a tiny electron transfer effect (see SI, Figure SI1). XPS further corroborates the hypothesis that DBT molecules are intact at RT. Indeed, as reported in Figure 2a, the Br 3d core level reveals the existence of almost exclusively carbon-bonded bromine (Br $3d_{5/2}$ BE= 69.7 eV).[20] Moreover, both the C 1s : Br 3d ratio (9.3 : 1) and the ratio between the different components of the C 1s peak, namely C-H : C-C : C-Br (5 : 3.2 : 1), are in agreement with the expected values for the intact molecules.

To study the thermo- and light-induced C-Br homolytic bond cleavage, we irradiate half of the surface of the Au single crystal at λ = 405 nm for 12 hours at RT. In this way a direct comparison of the effect of the annealing treatments on the two different areas is made possible.

Figure 1 reports the thermal behaviour of the non-illuminated area when the deposited monolayer (Figure 1a) is annealed at temperature lower than 410 K, no noticeable effects are observed while after treatments at 410 K (Figure 1b) the quality of the resulting surface is very poor, with partial desorption-decomposition of the DBT precursor. XPS analysis (Figure 2b) indicates a consistent coverage decrease (≈19%) with respect to the RT surface probably related to the low sublimation temperature of the precursor, as reported in the experimental section.

Little islands wherein molecules are ordered have been found sporadically. Figure 1c reports two of these areas formed by monomeric and dimeric species, the latter consisting of two tetracene units interconnected by a *bridging* bright dot and with two brighter *terminal* features at both sides of them (yellow circles in Figure 1c). Moreover, additional circular features are discernible in-between successive dimers (red circles in Figure 1c). According to literature data,[9,21] we propose that the observed monomers and dimers are formed by tetracene units, where bromine atoms have been substituted by gold atoms (yellow circles). The additional bumps between the molecules are the residual chemisorbed bromine (red circles), as visualized by the atomic model superimposed to the STM images (see also SI for optimized DFT monomeric and dimeric structures in Figures SI3a and SI4a, respectively). It is noteworthy that two chemisorbed bromine atoms laterally cap a couple of adjacent terminal (mono-coordinated) Au atoms belonging to successive dimers in a 1:1 ratio, while no bromine atoms are associated to the single bridging (twofold-coordinated) Au atom within each individual dimer. As a further proof of the organometallic nature of the dimers, STM analysis shows that the centre-to-centre distance within a dimer is 0.65±0.03 nm, significantly larger than the expected value for directly linked phenyl rings, e.g. nearest neighbour phenylene groups in poly(para-phenylene) (0.43 nm),[22] but in agreement with what expected for an organometallic structure.[12,23] Moreover, the lifted herringbone Au (111) reconstruction (see Figure 1b) suggests

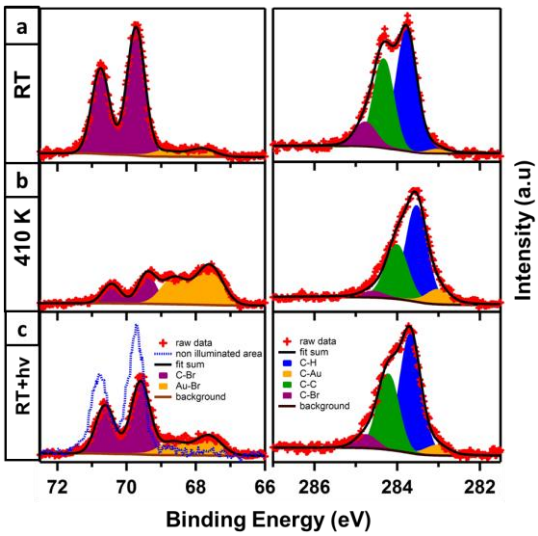

Figure 2: Br 3d (hv=150 eV) and C 1s (hv=400 eV) XPS spectra and fitting components of **a)** the DBT monolayer on Au (111); **b)** the DBT monolayer after annealing at 410 K; **c)** the DBT monolayer after illumination at RT. The blue dotted line in c) reports the Br 3d peak from the non-illuminated area of the same sample.

that the incorporated Au atoms are partially provided by surface reordering.[13]

C 1s XPS analysis further corroborates this scenario, since the area of the component at lower binding energy, usually associated to carbon bonded to metal atoms,[20,23] increases at the expense of the C-Br related peak: starting from 12%, the percentage of metal-bonded carbon (100·area$_{C\text{-}Au}$/ area$_{C\text{-}Au}$+ area$_{C\text{-}Br}$) becomes 74%, see Figure 2b. Moreover, the whole C 1s peak rigidly shifts towards lower BE (≈0.2 eV), as a consequence of both bromine chemisorption[24,25] and of lifting the herringbone reconstruction.[11]

Regarding the circular protrusions in-between the organometallic species, the XPS bromine spectra highlights the presence of mainly chemisorbed Br (Br 3d$_{5/2}$ BE 67.8 eV),[20] so we associate these features to chemisorbed bromine, as anticipated before. Finally, the DFT simulated images, based on the aforementioned model and on fully optimized atomic structures, well reproduces the experimental features, such as the brightness of Br side atoms (see inset in Figure 1a) and the contrast between the molecular cores and the surface adsorbed Br atoms (see inset in Figure 1c).

As observed for sterically hindered organic scaffolds,[12,26] the flat geometry of the DBT molecules maximizes the interaction with the Au (111) surface, but at the same time inhibits the metal elimination step of the Ullmann-like coupling reaction, so that the final C-C coupling is hampered. Even if at 410 K the C-Br bond is activated, the resulting organometallic network contains mainly dimeric and monomeric species while longer oligomers are randomly observed. Previous works[1,8] show that large organometallic islands of metal-interconnected monomers are usually obtained due to the reversible nature of the carbon-metal-carbon bonds, while for DBT this is not the case even after annealing at higher temperature. As reported in Figure 2b, the Br 3d area amounts to 53% of the as-deposited signal and only 27% is related to carbon-bonded bromine (14% of the initial amount), so that an incomplete de-bromination cannot justify the low polymerization degree. Even the availability of gold adatoms cannot justify this evidence, since longer oligomers require smaller amounts of metal atoms. A possible key to this behaviour is given by the presence of bromine atoms regularly lying adjacent to the terminal, mono-coordinated gold adatoms both in the dimers and in the monomers, which suggests that they contribute to the stabilization of these species.[6,27] In fact, DFT simulations show that gold adatoms singly-bonded to tetracene cores are electron-deficient, in the sense that a partial positive charge resides on them (see discussion in the SI and Figure SI2). For this reason chemisorbed Br atoms attractively interact with two neighbouring terminal Au atoms of gold-substituted tetracene molecules, thus stabilizing the formation of the ordered network. More precisely, our DFT calculation show that the experimental-like unit cell that contains two Br atoms is 0.4 eV more stable than the same cell without the bromines, which are assumed to adsorb far from the self-assembled structure in the latter case (see Figure SI3 and SI4 for details). We cannot exclude that other factors affect the observed outcome, such as the lattice mismatch between the surface and the periodicity of the oligomers, which could favour the formation of ordered island of dimers and monomers.

In summary, even if at 410 K the C-Br bond is activated, the quality of the resulting surface is very poor, with large disordered areas due to the partial desorption or decomposition of DBT molecules. By increasing the annealing temperature the quality of the resulting surface is even worse and the formation of direct C-C bonds is not observed, see Figure SI5.

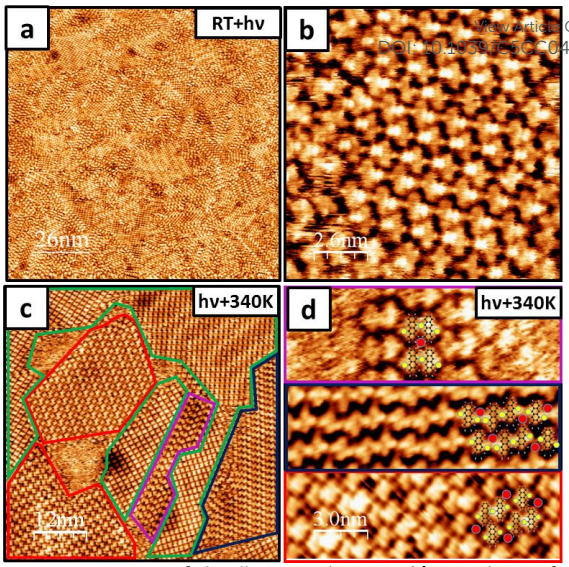

Figure 3: STM images of the illuminated area. **a-b)** monolayer of DBT molecules irradiated at RT; **c)** the same surface after annealing at 340 K. Islands with different ordered nanostructures are contoured with different colours; more precisely, the green islands are formed by brominated DBT while the red, blue and cyan islands by organometallic monomers or dimers. **d)** zoom-in of the islands formed by organometallic molecules. Tunneling parameters are a-b) I= 4 nA, V_{bias}= 0.99 V; b-c) I= 3.2 nA, V_{bias}= 0.52 V.

Moving to the illuminated area, reported in Figure 3, after the irradiation at RT (Figure 3a) we observe a strong variation of the topography: the herringbone reconstruction disappears within large area and the surface appears more disordered, even if the coverage does not change, i.e. the C 1s area is unaffected by the treatment. Figure 3b shows that, even if the as-deposited DBT molecules are still present, the majority of the surface is covered by organometallic species: indeed, bright dots as those observed after thermal activation of the precursors are clearly visible at the sides of the molecules. As before, when the bright dots appear, the underlying herringbone reconstruction is lifted, confirming that the bright dots are Au adatoms. Furthermore, the XPS analysis reveals the light-induced activation of the C-Br bond. Figure 2c reports the comparison of the Br 3d doublet measured on illuminated versus dark sample regions. Within the illuminated area the bromine signal is split in two components. Indeed, an additional Br 3d doublet appears at 67.8 and 68.8 eV accounting for 27% of the total signal area, indicating the presence of surface-stabilized bromine atoms.[20,28] The total subtended area decreases by 22% with respect to the dark sample regions, suggesting that part of the bromine desorbs during the irradiation and that the reaction yield is about 45%, see discussion below Figure SI6.

After a mild annealing at 340 K, unable to trigger the thermal dissociation of the C-Br bond (Figure SI6), the order of the illuminated area is strongly enhanced, as shown in Figure 3c. The dark area, instead, is unaffected by this treatment since only the as-deposited structure is observed. In the illuminated area two types of ordered islands are well distinguishable: the one above the Au

(111) herringbone reconstructed surface (contoured with green lines in Figure 3c), where the as-deposited DBT structure is still present, and those on the un-reconstructed surface (contoured with red, blue and cyan lines in Figure 3c and 3d), where different ordered nanostructures of organometallic monomers and dimers are visible according to the different bonding scheme obtainable from the asymmetric functionalization of the tetracene core. These organometallic ordered structures are the same that are obtained with an annealing at 410 K: the main difference is that the coverage does not decrease and the order is strongly improved due to the low temperature treatment in the light-triggered surface reaction. Remarkably, even with this light-triggered procedure longer oligomeric chains are not formed. As the temperature is increased above 410 K, the illuminated and dark regions become microscopically and spectroscopically indistinguishable, with a decrease of the coverage and of the structural order.

In summary, by combining UHV-STM, XPS and DFT we have shown that a light stimulus can be used to trigger the first step of the Ullmann coupling reaction. In particular, the irradiation procedure leads to the C-Br bond cleavage at RT rather than at 410 K, thus allowing one to obtain a completely ordered organometallic network after a mild annealing. Since it has to be noted that the light-induced debromination in gas-phase occurs at shorter wavelengths, it appears reasonable then to imagine an active role of the substrate in the observed reactivity by mean the known indirect excitation process.[29] Our precursor (5,11-dibromo-tetracene) cannot further react due to sterical hindering between the units. For this reason differently functionalized molecules will be studied to highlight the differences between thermal and photochemical activation in sterical conditions allowing for Ullmann coupling completion. An orthogonal activation of the polymerization with respect to the extensively applied thermal treatments may be of particular interest to improve the quality of the covalent organic networks. In this sense, a light-triggered C-Br dissociation offers a new possible way to combine halogens with other functional groups to exploit a hierarchical synthesis, wherein sequential light and thermal treatments may be applied to polymerize a bi-functional precursor.

This work has been partially funded by MIUR (PRIN 2010/11, Project No. 2010BNZ3F2: “DESCARTES”), Progetti di Ricerca di Ateneo (CPDA118475/11), Progetto Futuro in Ricerca 2012 (RBFR128BEC) and by CINECA supercomputing center through LI03p_CBC4FC and IscrB_CMGEC4FC grants.

Notes and references

1 Q. Fan, C. Wang, Y. Han, J. Zhu, W. Hieringer, J. Kuttner, G. Hilt, J. M. Gottfried, *Angew. Chem. Int. Ed. Engl.* **2013**, 52, 4668–72.

2 J. Cai, P. Ruffieux, R. Jaafar, M. Bieri, T. Braun, S. Blankenburg, M. Muoth, A. P. Seitsonen, M. Saleh, X. Feng, et al., *Nature* **2010**, 466, 470–3.

3 F. Sedona, M. Di Marino, M. Sambi, T. Carofiglio, E. Lubian, M. Casarin, E. Tondello, *ACS Nano* **2010**, 4, 5147–54.

4 R. Lindner, A. Kühnle, *ChemPhysChem* **2015**, DOI: 10.1002/cphc.201500161.

5 L. Lafferentz, V. Eberhardt, C. Dri, C. Africh, G. Comelli, F. Esch, S. Hecht, L. Grill, *Nat. Chem.* **2012**, 4, 215–20.

6 J. Park, K. Y. Kim, K. H. Chung, J. K. Yoon, H. Kim, S. H. S. J. Kahng, *J. Phys. Chem. C* **2011**, 115, 14834–14838.

7 W. Wang, X. Shi, S. Wang, M. a Van Hove, N. Lin, *J. Am. Chem. Soc.* **2011**, 133, 13264–7.

8 M. Bieri, S. Blankenburg, M. Kivala, C. a Pignedoli, P. Ruffieux, K. Müllen, R. Fasel, *Chem. Commun. (Camb)*. **2011**, 47, 10239–41.

9 J. Eichhorn, D. Nieckarz, O. Ochs, D. Samanta, M. Schmittel, P. J. Szabelski, M. Lackinger, *ACS Nano* **2014**, 8, 7880–9.

10 Q. Fan, C. Wang, L. Liu, Y. Han, J. Zhao, J. Zhu, J. Kuttner, G. Hilt, J. M. Gottfried, *J. Phys. Chem. C* **2014**, 118, 13018–13025.

11 A. Basagni, F. Sedona, C. A. Pignedoli, M. Cattelan, L. Nicolas, M. Casarin, M. Sambi, *J. Am. Chem. Soc.* **2015**, 137, 1802–1808.

12 A. Saywell, W. Greń, G. Franc, A. Gourdon, X. Bouju, L. Grill, *J. Phys. Chem. C* **2014**, 118, 1719–1728.

13 H. Zhang, J. H. Franke, D. Zhong, Y. Li, A. Timmer, O. D. Arado, H. Mönig, H. Wang, L. Chi, Z. Wang, et al., *Small* **2014**, 10, 1361–1368.

14 J. Björk, F. Hanke, S. Stafström, *J. Am. Chem. Soc.* **2013**, 135, 5768–75.

15 A. Basagni, L. Colazzo, F. Sedona, M. DiMarino, T. Carofiglio, E. Lubian, D. Forrer, A. Vittadini, M. Casarin, A. Verdini, et al., *Chemistry* **2014**, 20, 14296–304.

16 H. Y. Gao, D. Zhong, H. Mönig, H. Wagner, P. A. Held, A. Timmer, A. Studer, H. Fuchs, *J. Phys. Chem. C* **2014**, 118, 6272–6277.

17 Q. Shen, J. H. He, J. L. Zhang, K. Wu, G. Q. Xu, A. T. S. Wee, W. Chen, *J. Chem. Phys.* **2015**, 142, 101902.

18 K.-H. Chung, B.-G. Koo, H. Kim, J. K. Yoon, J.-H. Kim, Y.-K. Kwon, S.-J. Kahng, *Phys. Chem. Chem. Phys.* **2012**, 14, 7304–8.

19 T. A. Pham, F. Song, M.-T. Nguyen, M. Stöhr, *Chem. Commun. (Camb).* **2014**, 50, 14089–14092.

20 K. A. Simonov, N. A. Vinogradov, A. S. Vinogradov, A. V Generalov, E. M. Zagrebina, N. Mårtensson, A. A. Cafolla, T. Carpy, J. P. Cunniffe, A. B. Preobrajenski, *J. Phys. Chem. C* **2014**, 118, 12532–12540.

21 J. Eichhorn, T. Strunskus, A. Rastgoo-Lahrood, D. Samanta, M. Schmittel, M. Lackinger, *Chem. Commun. (Camb).* **2014**, 50, 7680–2.

22 J. a Lipton-Duffin, O. Ivasenko, D. F. Perepichka, F. Rosei, *Small* **2009**, 5, 592–7.

23 M. Di Giovannantonio, M. El Garah, J. Lipton-Duffin, V. Meunier, L. Cardenas, Y. Fagot Revurat, A. Cossaro, A. Verdini, D. F. Perepichka, F. Rosei, et al., *ACS Nano* **2013**, 7, 8190–8198.

24 A. Batra, D. Cvetko, G. Kladnik, O. Adak, C. Cardoso, A. Ferretti, D. Prezzi, E. Molinari, A. Morgante, L. Venkataraman, *Chem. Sci.* **2014**, *5*, 4419–4423.

25 M. Chen, J. Xiao, H. P. Steinrück, S. Wang, W. Wang, N Lin, W. Hieringer, J. M. Gottfried, *J. Phys. Chem. C* **2014** 118, 6820–6830.

26 L. Ferrighi, I. Píš, T. H. Nguyen, M. Cattelan, S. Nappini, A. Basagni, M. Parravicini, A. Papagni, F. Sedona, E. Magnano, et al., *Chem. - A Eur. J.* **2015**, 21, 5826–5835.

27 H. Zhang, H. Lin, K. Sun, L. Chen, Y. Zagranyarski, N. Aghdassi, S. Duhm, Q. Li, D. Zhong, Y. Li, et al., *J. Am. Chem. Soc.* **2015**, 137, 4022–4025.

28 A. Lunghi, F. Totti, *J. Mater. Chem. C* **2014**, 2, 8333–8343.

29 J. Lee, S. Ryu, J. Chang, S. Kim, S. K. Kim, *J. Phys. Chem. B* **2005**, 109, 14481–5.